This is a preprint of the following article, which is available from mdolab.engin.umich.edu
Fouda, M., Adler, E. J., Bussemaker, J. H., Martins, J. R. R. A., Kurtulus, D. F., Boggero, L., Nagel, B., Automated Hybrid Propulsion Model Construction for Conceptual Aircraft Design and Optimization. *Congress of the International Council of the Aeronautical Sciences (ICAS 2022)*, September 2022, Stockholm, Sweden.
The published article may differ from this preprint.

Automated Hybrid Propulsion Model Construction for Conceptual Aircraft Design and Optimization

Mahmoud Fouda[1], Eytan J. Adler[2], Jasper H. Bussemaker[1], Joaquim R.R.A. Martins[2], D.F. Kurtulus[3], Luca Boggero[1], and Björn Nagel[1]
[1]*DLR (German Aerospace Center), Institute of System Architectures in Aeronautics, Hamburg, Germany*
[2]*University of Michigan, Ann Arbor, Michigan, USA*
[3]*Middle East Technical University, Ankara, Turkey*

Abstract

Electric and hybrid-electric propulsion systems are key technologies for sustainable aviation. Electric propulsion systems introduce many design possibilities, which must be considered in the conceptual design stage to take full advantage of electrification. This makes for a challenging conceptual design problem. Architecture optimization can be applied to explore large design spaces and automatically find the best architectures for a set of requirements. Electric propulsion architecture optimization requires automated and flexible propulsion system modeling. It also requires the analysis of the propulsion architecture at an aircraft level to compute a meaningful objective function for the optimization. In this study, we present an approach for defining the propulsion system architectures and evaluating their aircraft-level performance. A propulsion architecture is defined using a modular interface, allowing architectures to be automatically evaluated on the aircraft-level for a predefined mission. OpenConcept, an open source conceptual design and optimization toolkit, is used to implement the multidisciplinary problem. We present a case study of the electrification of a regional transport aircraft Beechcraft King Air C90GT with automated definition, integration and evaluation of five different propulsion systems. We perform multidisciplinary design optimization to minimize fuel burn and maximum takeoff weight for a sweep of design ranges and battery specific energies. Our approach opens the door to electric propulsion architecture optimization.

1 Introduction

Aviation contributes 3–4% of the net anthropogenic climate impact [12], and this value will increase as other sectors decarbonize. The European Union, ICAO, IATA, and NASA have set aggressive targets to reduce aviation's contribution to climate change [1, 4]. An enabling technology to help meet these goals is electrification, which can reduce or even eliminate the operational emissions of short-range aircraft. Electric technologies introduce new propulsion system and aircraft configuration possibilities. The vast number of possibilities raises an important question: how can conceptual designers consider so many options when designing an aircraft for a specific application?

1.1 Challenges in Electric Propulsion System Design

Electrification allows increases in the number of propulsors and their placement, due in part to the scaling properties of electric motors [3]. The introduction of electric components and connection strategies enables new architectures that need to be considered early in the design process [13]. In addition, electric aircraft design is a multidisciplinary design problem due to close coupling between engineering disciplines. This means any division of the design process is not possible because a change in one discipline could produce strong effects in other domains. This makes the definition of parameters and the coupled subsystem analysis a challenging endeavor [14]. The close coupling between aerodynamics, propulsion and thermal management in the design of electric systems is a major challenge for existing analysis environments [3].

The large design space and necessity for subsystem integration limit the designer's capability to consider most architectures in the conceptual design stage. While it would be beneficial to reduce subjectivity by considering all architecture choices, the automation of the design optimization process is a major barrier. Each architecture must be manually defined and integrated into the aircraft model. Designers must either reduce the design space using engineering intuition, leading to expert bias and subjectivity [8], or spend time and resources performing repetitive tasks related to architecture definition and integration. Thus, designers need a flexible and rapid construction of propulsion architecture models as a starting point for overall vehicle integration and performance evaluation. This would automate design space exploration efforts.

1.2 Propulsion Architecture Optimization

Architecture optimization enables the automated search for best candidate architectures in the early phase of design [7]. Since electric aircraft design has many degrees of freedom, it is not possible to perform a manual search for best architectures with a given set of possible architecture choices. Architecture optimization defines the design problem as a numerical optimization problem, enabling automated conceptual design space exploration studies for propulsion system architectures. Implementing architecture optimization requires the ability to quantitatively evaluate candidate architectures [5]. Therefore, the introduction of a modular interface for propulsion architecture definition and quantitative evaluation is the first step needed for electric propulsion architecture optimization.

This paper extends the work presented in [3] by automating the propulsion architecture definition and integration into the aircraft model for mission analysis. It focuses on the initial methodology and work flow setup needed as a prerequisite for architecture optimization. We perform a case study: designing an electrified King Air C90GT regional transport aircraft. The paper first describes the method used to define a propulsion system and perform aircraft-level evaluation. Next, we present the optimization problem formulation and the case study results. The final section contains conclusions and future work.

2 Methodology

To build a framework for automated architecture evaluation, we develop a propulsion system architecting module and combine it with an existing mission analysis toolkit called OpenConcept[1]. The architecting module handles the propulsion system definition and construction. We define a reference aircraft model that automatically integrates the propulsion system with aerodynamics and

[1] github.com/mdolab/openconcept

weight models. OpenConcept then performs a mission analysis of the aircraft model to compute objectives such as fuel burn and energy usage for the specified propulsion system.

2.1 Propulsion System Architecture and Components

The propulsion system consists of high-level components, such as propellers and electric motors, that interact to provide propulsive power [9]. The numerical models of the constituent components and the flow of information among them represent the propulsion architecture.

A set of conceptual-level electrical, mechanical, and turbomachinery components from OpenConcept are used to model the propulsion system. The components are connected together to form propulsion architecture configurations (e.g., turboelectric and series hybrid), described in Figure 1. The list of currently available OpenConcept propulsion system components that are extended in the current study includes

- Motor: generates shaft power by drawing electric load
- Generator: transforms shaft power into electric AC power
- Converter: converts AC to DC power as a rectifier or DC to AC power as an inverter
- Bus: distributes power or loads
- Battery: provides electric DC power with constant specific energy and specific power
- Turboshaft: provides mechanical power from fuel; assumes a constant power specific fuel consumption (PSFC)
- Gearbox: reduces rotational speed with a variable efficiency loss
- Propeller: converts shaft power to thrust based on an efficiency map
- Splitter: splits power or loads into two outputs

Each component has one or more sizing variables. Default values are assigned to the inputs that represent the current state of the art and can be overridden by the user.

2.2 Propulsion Architecture Builder

The architecture builder connects components to produce a given architecture that can be integrated into an aircraft model. It defines a set of classes that describes and constructs the propulsion system. The classes divide the system into three sets of architecture elements:

- Thrust generation elements: convert shaft power to thrust
- Mechanical Power generation elements: generate mechanical shaft power from fuel or electric DC power
- (Optional) Electric power generation elements: provide electric DC power from battery or an engine chain (e.g., engine + generator + rectifier); this group is only needed if electric DC power is required for mechanical shaft power generation.

The three element groups provide a complete description of the propulsion system architectures. A more detailed description of these groups follows.

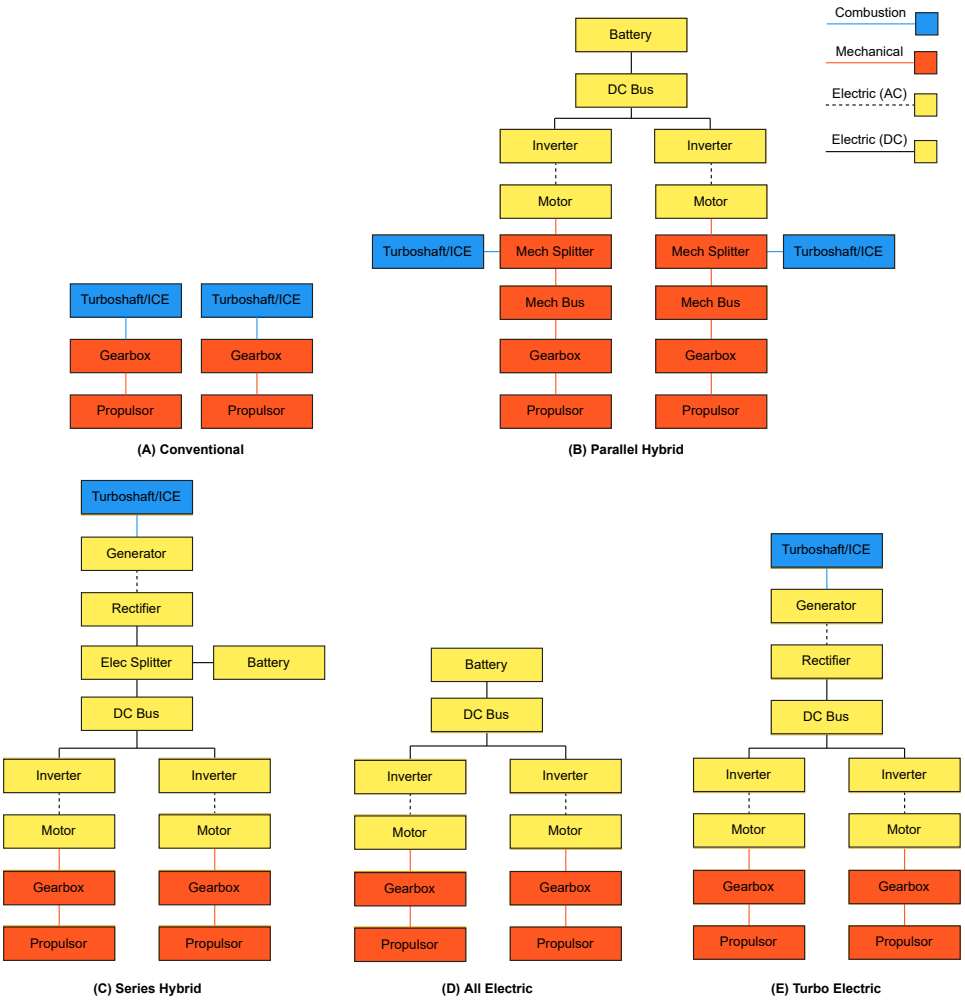

Figure 1: Notional propulsion system architectures. Di erent propulsion system architectures are made by adding, removing, or rearranging propulsion system components.

Thrust generation elements are the first building block of the description of a propulsion architecture. They contain a group of components that receive shaft power and convert it to thrust. These components are a propeller and (optionally) a gearbox.

Mechanical power generation elements receive either fuel or electric DC power and generate shaft power. Three different subgroup options are available: a conventional turboshaft engine, an electric motor, or a combination of both. In the context of this group, the degree of hybridization (DoH) describes the ratio of shaft power generated by the electric motor (if it exists) to the total generated shaft power. The throttle input is applied to the total power available. For example for a series hybrid architecture, the throttle is applied on the rated power of the electric motor. In the case of a parallel hybrid architecture, the throttle is applied on the sum of the rated powers of the turboshaft engine and the electric motor.

Electric power generation elements provide electric DC power from a battery or engine chain. This stage is only included if electrical power is needed by the mechanical power generation elements. Two subgroup options are available that combine into three possible configurations: a battery, an engine chain with a generator and a rectifier, or a combination of the two. In the context of this

group, the degree of hybridization (DoH) is the ratio of electrical power generated by the battery to the total generated electrical power.

The elements are connected based on a function decomposition of the propulsion system components. This allows the user to define a propulsion system by passing only the components within each of the three groups. The architecture builder will automatically connect them to form the propulsion system model. The logic for connecting the components is illustrated in Figure 2. A detailed description of the power train design of the parallel and series hybrid architectures including the implementation of the One Engine Inoperative (OEI) is presented in the Appendix in Figures 12, 13 and 14.

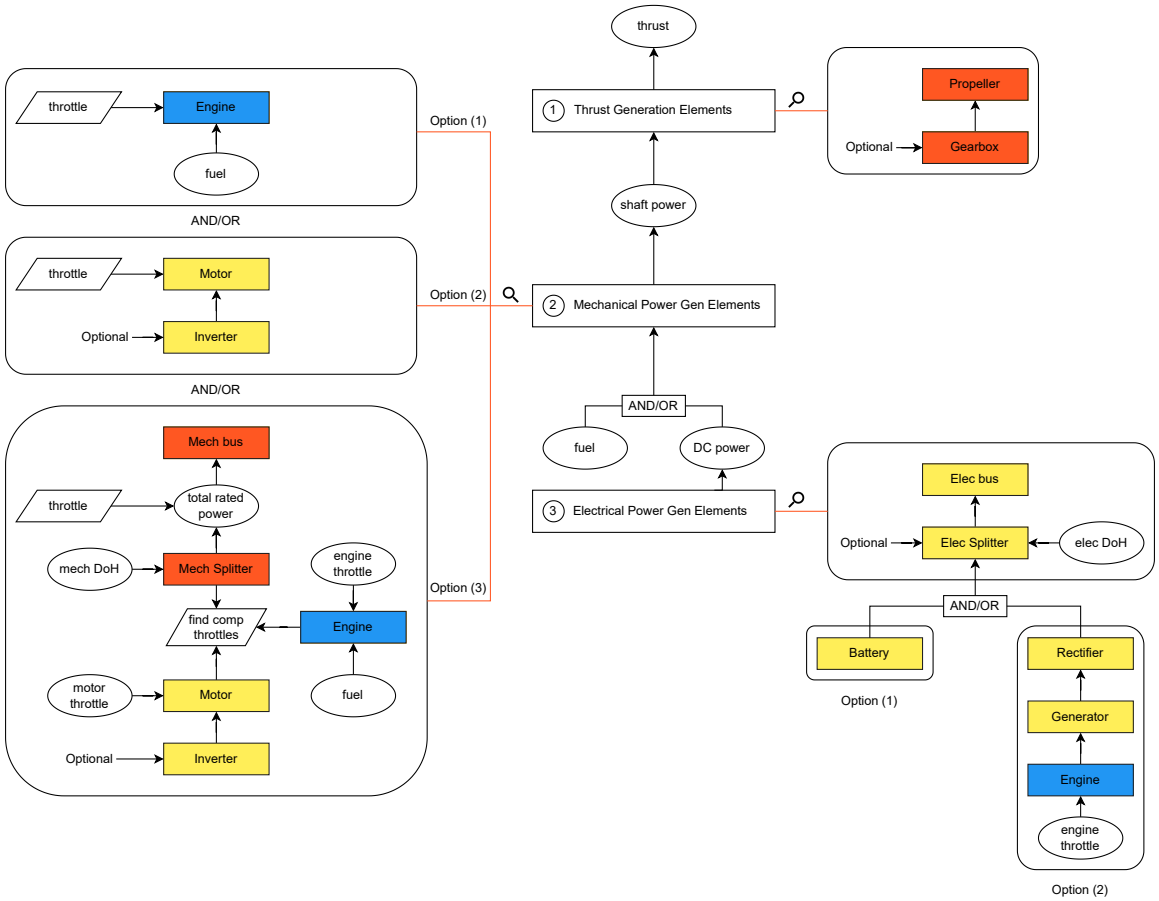

Figure 2: Architecture builder logic. The builder uses a function-based decomposition to construct the propulsion system from propulsion system components. For example, thrust generation elements have a thrust group that is composed of a propeller and gearbox as a unit that can be repeated to produce single or twin-prop architectures. Mechanical power generation has 3 di erent possible mechanical groups that can be used to generate shaft power.

The architecture builder is extensible; additional components can be added to allow for even more propulsion systems. For example, a fan could be added to the thrust generation elements group as an alternative for propellers. Furthermore, new connection logic can also be added. For example, the current version of the builder only considers DC transmission architectures, as they are more advantageous for hybrid electric propulsion [16]. However, the builder can be extended to allow AC architecture connections by adding an option with only an electric motor in the mechanical power generation group and another option of an engine chain without a rectifier in the electric power group. The current implementation of the architecture builder allows the definition of architectures

with any number of propellers. Therefore, it can be used to construct distributed propulsion architectures with either all electric, turboelectric, or series hybrid configurations.

2.3 Aircraft-Level Architecture Evaluation

Aircraft-level mission analysis gives a realistic estimate of the performance of a given propulsion system architecture. The fuel burn, takeoff weight, and energy usage during the mission depend on the propulsion system efficiency, aircraft weight, aerodynamic efficiency. The propulsion system efficiency contributes to battery and fuel weight. The battery, fuel, and propulsion system weight add to the aircraft weight. This introduces coupling between the objective function (e.g., fuel burn, takeoff weight, or energy usage) and the propulsion system design. A converged mission analysis returns the takeoff weight, fuel burn, and energy usage, and can be extended to compute other quantities, such as cost per nautical mile. These outputs are used to compare the performance of different propulsion architectures.

3 Implementation

We use NASA's OpenMDAO framework [11] to automatically create the numerical model and control the flow of information between the different models within the aircraft. OpenMDAO is an open source, object oriented multidisciplinary design optimization (MDO) framework written in Python. OpenConcept [3], a conceptual aircraft design and optimization toolkit, is coupled to our architecting module to enable mission simulation and overall aircraft design. The architecting module dynamically constructs the propulsion system model used by OpenConcept.

3.1 OpenConcept

OpenConcept is a software toolkit originally developed for mission analysis of electric and hybrid-electric fixed-wing aircraft [3]. It is built using the OpenMDAO framework [11] developed at NASA, which facilitates automated coupling of multidisciplinary analysis blocks and system-level analytic gradient computation. OpenConcept uses these analytic derivatives to enable rapid problem convergence with gradient-based solvers and efficient gradient-based optimization. For this work, OpenConcept is used to

- model the propulsion system components and aircraft aerodynamics and
- provide the numerical framework for mission analysis, including a numerical integrator and mission profile module.

An OpenConcept aircraft model takes in aircraft design variables (e.g. wing area and propulsion system sizing variables), throttle position, lift coefficient, and flight conditions, and outputs thrust, weight and drag. The aircraft design variables are assumed to start at default values that match the reference aircraft model, including the operating empty weight. The architecture builder assembles the propulsion system that is used in the aircraft model. A parabolic drag polar, based on parameters from the reference aircraft model, is used to compute the drag.

This work uses OpenConcept's `FullMissionAnalysis` mission profile. It includes takeoff, climb, cruise, and descent segments. The takeoff segment performs a balanced field length calculation, the details of which are described by Brelje [3]. The climb, cruise, and descent segments assume steady flight, which is achieved by solving for the throttle setting and lift coefficient such that the horizontal and vertical accelerations are zero at each integration point in the mission. The climb and descent segments use a predefined profile, determined by a set airspeed and vertical speed. The

length of the cruise segment is then set such that the total mission range meets the value input by the user. A Newton solver converges this system.

OpenConcept's numerical integration scheme uses Simpson's Rule to integrate state variables with an all-at-once approach. For performance, OpenConcept uses vectorized computations in each mission segment. This means that time-marching ordinary differential equation integration approaches cannot be used because vectorized quantities must be computed all at once. The integrator integrates necessary variables, such as fuel flow and airspeed, to compute quantities needed for the mission analysis, such as fuel weight and distance flown, respectively. The integrator can also be used in combination with OpenConcept components to enable novel analyses, including time-accurate battery temperature modeling and unsteady thermal management system analysis [2].

3.2 Architecture Builder Module

The architecture builder UML diagram is presented in Figure 3. It consists of two parts. The first part is the `PropSysArch` class that describes the propulsion system, its constituent components, and the relationships among them. The second is the `DynamicPropulsionArchitecture` OpenMDAO group, which constructs the propulsion system model hierarchy in a format that can be used by OpenConcept. Each propulsion system component is defined as a data class that contains its inputs and attributes, while its underlying numerical model is provided by OpenConcept. This step is necessary to provide the flexibility to change the numerical model for different levels of fidelity.

The `PropSysArch` class has three building blocks, called architecture elements: thrust generation elements, mechanical power generation elements, and electric power generation elements (described in Section 2.2). A user inputs the constituent components of these elements, and the dynamic builder automatically constructs an OpenConcept propulsion architecture model. `PropSysArch` calls `create_thrust_groups` and `create_mech_group` to connect the components in the thrust generation and mechanical power generation groups, respectively. `create_mech_group` returns a boolean that specifies whether electric power generation is needed, which is used to determine whether to call `create_electric_group` to add electric power generation components.

3.3 Multidisciplinary Analysis

Finally, we need to combine the elements to create an aircraft model that can be used by OpenConcept for mission analysis. We define a reference aircraft with aerodynamic and weight models and a propulsion system via the architecture builder. The propulsion system is then added to the aircraft model. Lastly, the sizing optimizer called with the necessary design variables and constraints for each propulsion architecture.

The propulsion system variables, such as electric motor specific power, are assigned default values that represent the current state of the art. The zero-lift drag coefficient, C_{D0}, and the maximum lift coefficient $C_{L,\,max}$ are assumed to match the reference aircraft model. The output of a successful mission analysis (i.e., the converged multidisciplinary problem) provides the performance evaluation metrics for a given propulsion architecture at an aircraft level. These performance metrics include maximum takeoff weight (MTOW), fuel burn, and energy usage.

4 Case Study: Electrification of a King Air C90GT

Five different propulsion architectures are used as examples to demonstrate the capabilities of our framework and modeling approach. The architectures are visualized in Figure 1 and include

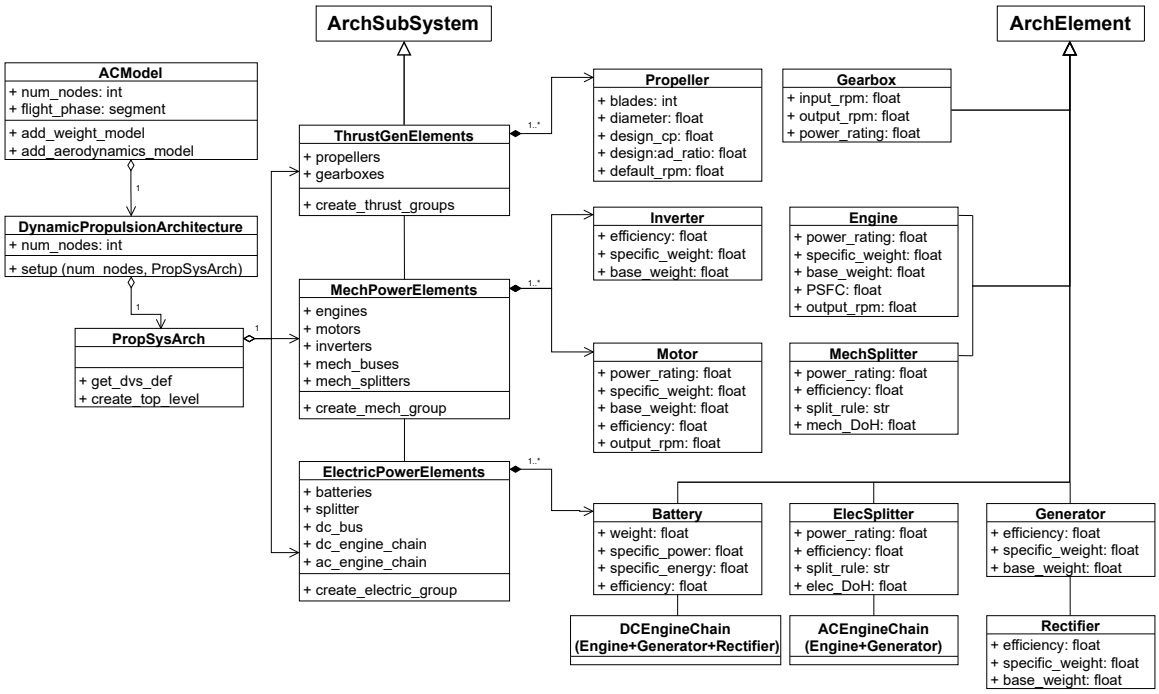

Figure 3: Architecture builder UML diagram. The architecture builder constructs the propulsion system from thrust, mechanical power, and electrical power generation elements. Each of these contains propulsion system components that are be grouped together (e.g., a gearbox to a propeller to generate thrust from shaft power). The construction logic is added as class methods under the relevant elements. By passing the component information to the builder, it can automatically construct an OpenConcept propulsion architecture model.

conventional, all electric, turboelectric, series hybrid, and parallel hybrid twin propulsion systems. All are twin-propeller systems to match the King Air. We test each architecture at different mission ranges and battery specific energies. Specific power and efficiency assumptions are stated in Table 1. Each optimization, i.e. an architecture evaluation, runs in approximately 2 minutes on a typical notebook PC. The authors would like to point out that *the aim of the present study is neither to prove nor disprove the viability of electric propulsion* for light aircraft retrofit design, but rather to demonstrate an automated approach to allow rapid integration and evaluation of different propulsion architectures into a conceptual design and optimization framework.

Table 1: Powertrain technology assumptions

Component	Specific Power (kW/kg)	Efficiency	PSFC (lb/hp/hr)
Battery	5.0	97%	-
Motor	5.0	97%	-
Generator	5.0	97%	-
Converter	10.0	97%	-
ElecBus	-	99%	-
Turboshaft	7.15[2]	-	0.6
MechBus	-	95%	-

[2] does not include 104 kg base wt

4.1 Optimization Problem

We use the SNOPT optimizer [10] through OpenMDAO's pyOptSparse [15] wrapper. We include design variables for the propulsion system components (rated powers of the turboshaft engine and/or electric motor), MTOW, battery weight, propeller diameter, and degree of hybridization (DoH) in cruise. The wing loading is held constant to match the reference aircraft stall requirements by varying the wing area as MTOW changes.

Constraints on the turboshaft, electric motor, and battery are added to ensure they do not exceed their rated power outputs. Battery specific power, p_b, is set to 5 kW/kg and battery specific energy is varied from 300–800 Wh/kg. An upper bound on MTOW of 5,700 kg is applied to prevent the takeoff weight from vastly exceeding reference aircraft model's MTOW. Additionally, EASA and the FAA require pilots to obtain a type rating to fly aircraft with MTOW above 5,700 kg.

The objective is selected to be suitable for all architectures by minimizing fuel burn, then minimizing MTOW when fuel burn is zero. The coefficient on MTOW in the objective function is on the order of the ratio between the energy densities of batteries and fuel (the energy density of aviation fuel is roughly 12,000 Wh/kg). The most general case of the optimization problem is as follows:

minimize:	fuel burn + $0.01MTOW$
by varying:	
	$MTOW$
	d_{prop}
	$W_{battery}$
	P_{motor} (rated)
	$P_{turboshaft}$ (rated)
	DoH_{cruise} (degree of hybridization w.r.t power at cruise)
subject to scalar constraints:	
	$R_{TOW} = W_{TO}$ - W_{fuel} - W_{empty} - $W_{payload}$ - $W_{batt} \geq 0$
	$SOC_{batt} \geq 0$ (battery's state of charge at the end of the mission)
	BFL $\leq$ 4,452 ft (no worse than baseline)
and vector constraints:	
	$0 \leq throttle \leq 1$
	$\overrightarrow{P}_{motor} \leq P_{motor}$ (rated)
	$\overrightarrow{P}_{turboshaft} \leq P_{turboshaft}$ (rated)
	$\overrightarrow{P}_{battery} \leq W_{battery} \cdot p_b$

Design variables and constraints are excluded from the optimization problem based on the propulsion architecture passed by the user. For example, if the architecture includes a battery, the battery weight is added as a design variable and the battery energy and power usages are constrained. This strategy allows a dynamic construction of the optimization problem based on the specified architecture, which is necessary for architecture optimization studies.

4.2 Architecture MDO Results

The validation for the conceptual model of the reference aircraft is performed in [3].For each propulsion architecture, we run a grid of 121 combinations of mission range and battery specific energy from 300 to 800 nmi and Wh/kg, respectively, with a step size of 50. Conventional and turboelectric architectures have no battery, and thus are optimized only on a sweep of mission ranges and not battery specific energies.

4.2.1 Conventional and Turboelectric Architectures

For the conventional and turboelectric architectures, the optimizer sizes the turboshaft rated power. The highest conventional architecture MTOW of 3,576 kg (shown in Figure 4b) occurs at the maximum range of 800 nmi. This weight is 26% less than the turboelectric configuration's MTOW of 4,838 kg at the same point, as shown in Figure 5b. This is due to the extra weight needed for the generator, converters, motors, and additional structure. The replacement of the conventional architecture with a turboelectric architecture at this design point leads to an increase in fuel burn of 50% (from 491 kg to 743 kg), corresponding to energy consumptions of 5,867 kWh and 8,883 kWh respectively (shown in Figures 4d and 5d). This is caused in part by the additional weight and in part by the reduced efficiency of the propulsion system because of the additional energy conversion losses.

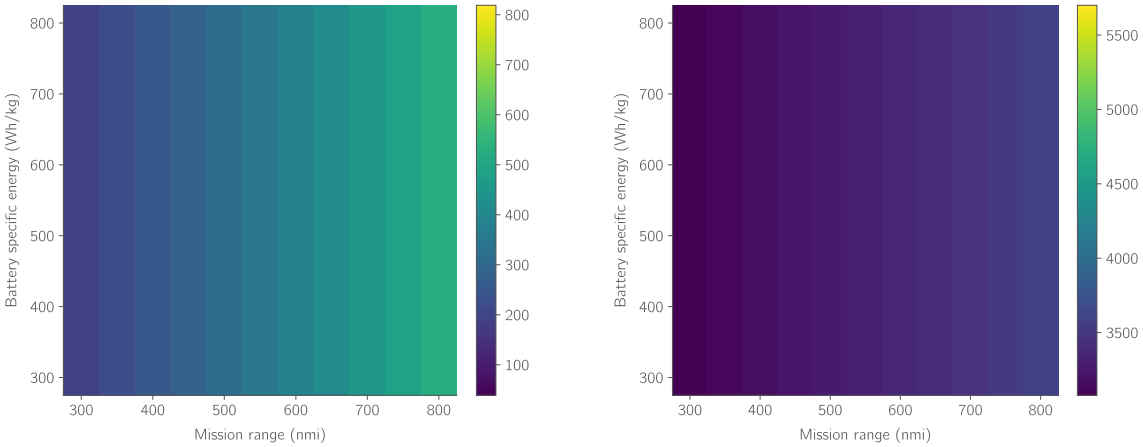

(a) Fuel burn + MTOW / 100 (kg)

(b) MTOW (kg)

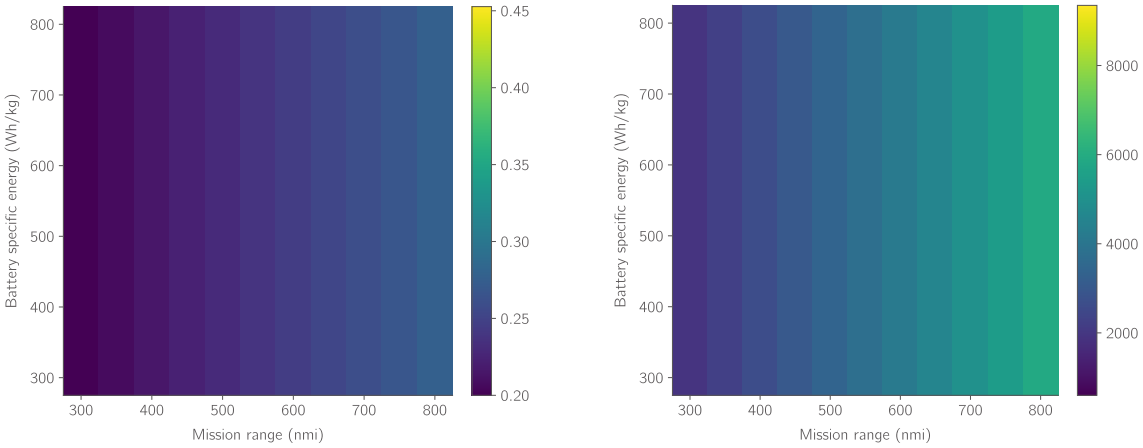

(c) $W_{PropSys}$ (including fuel and battery) / MTOW

(d) Energy used (kWh)

Figure 4: Conventional architecture MDO results.

The total weight fraction of the propulsion system, including fuel, increases from 30% for the conventional architecture to 40% for the same turboelectric case. These results reflect the expected result that the turboelectric architecture performs worse than the conventional architecture when no aerodynamic or propulsive efficiency benefits (such as distributed electric propulsion) are added. There is a clear shift from Figure 4 to Figure 5 toward more weight and higher energy consumption

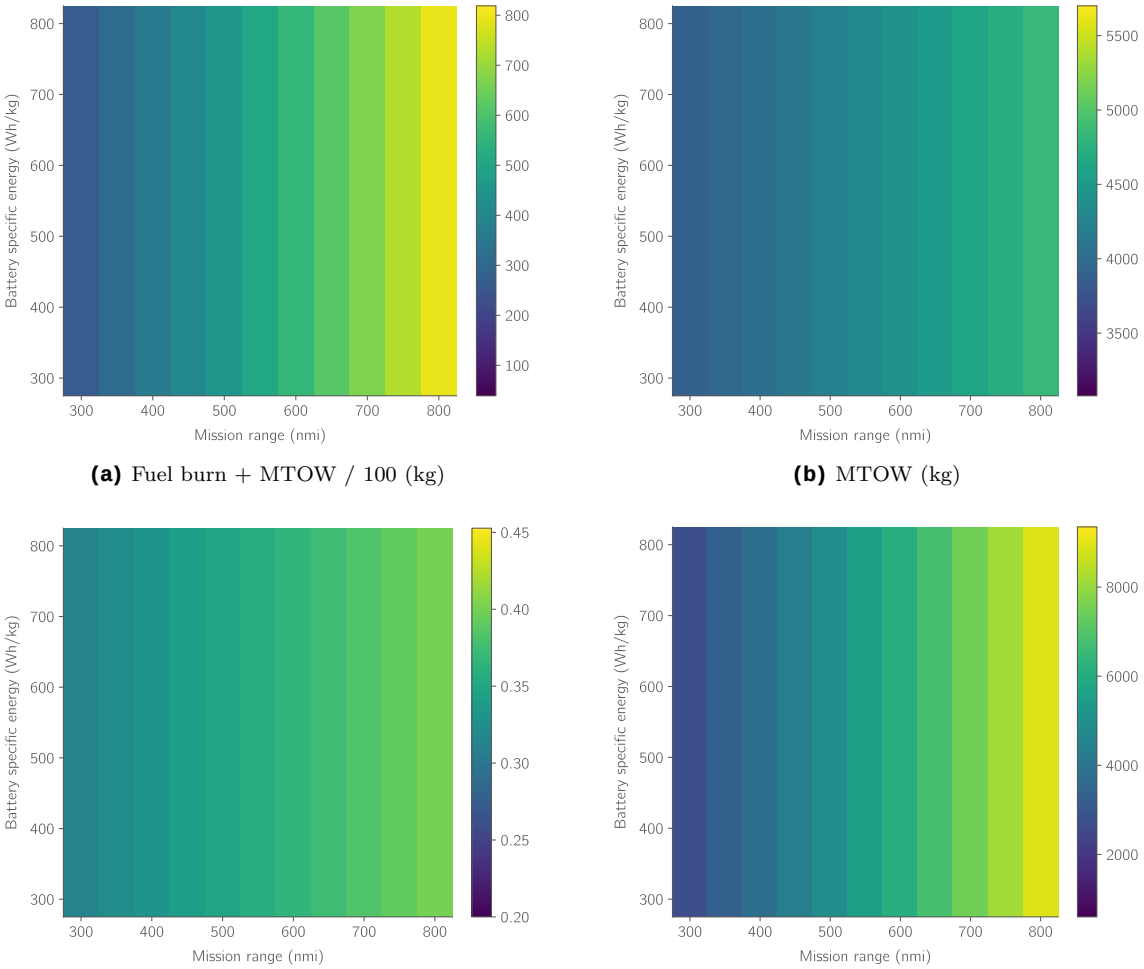

(a) Fuel burn + MTOW / 100 (kg)

(b) MTOW (kg)

(c) $W_{PropSys}$ (including fuel and battery) / MTOW

(d) Energy used (kWh)

Figure 5: Turboelectric architecture MDO results.

at all design points.

4.2.2 All Electric Architecture

For the all electric architecture, only 21 cases have successfully converged. In the infeasible (white) region in Figure 6, there is no possible combination of design variables that allows the aircraft to fly the mission while staying under the MTOW and component power output constraints. At 350 nmi and 550 Wh/kg, the design has a MTOW of 5,516 kg which is only 184 kg below the upper bound. Any further increase in range requires an improvement in battery specific energy. At a range of 300 nmi and battery specific energy of 500 Wh/kg the all electric design has an MTOW of 5,212 kg (shown in Figure 6b, a 69% increase in weight compared to the conventional architecture at the same point. The propulsion system, including the battery, accounts for more than 40% of the total takeoff weight. Even at a highly optimistic assumption of 800 Wh/kg and a short range of 300 nmi, the all electric configuration has a high takeoff weight of 3,908 kg. This is only 14% less than the reference aircraft model's weight of 4,581 kg, which is designed to fly 1,000 nmi.

The assumed value of battery specific energy, e_b, significantly affects the sizing of the aircraft model. At a range of 400 nmi, increasing battery specific energy from the first converged case

of 650 Wh/kg decreases MTOW, with values of 5,347, 5,014, 4,756, and 4,551 kg. However, the decrease is nonlinear with respect to the increase in e_b. The reduction in weight due to higher e_b declines as one moves upward on the vertical axis of Figure 6b. As it makes up a large component of takeoff weight, the battery weight from Figure 6d follows the same trend, with weights of 1,665, 1,452, 1,288, and 1,158 kg.

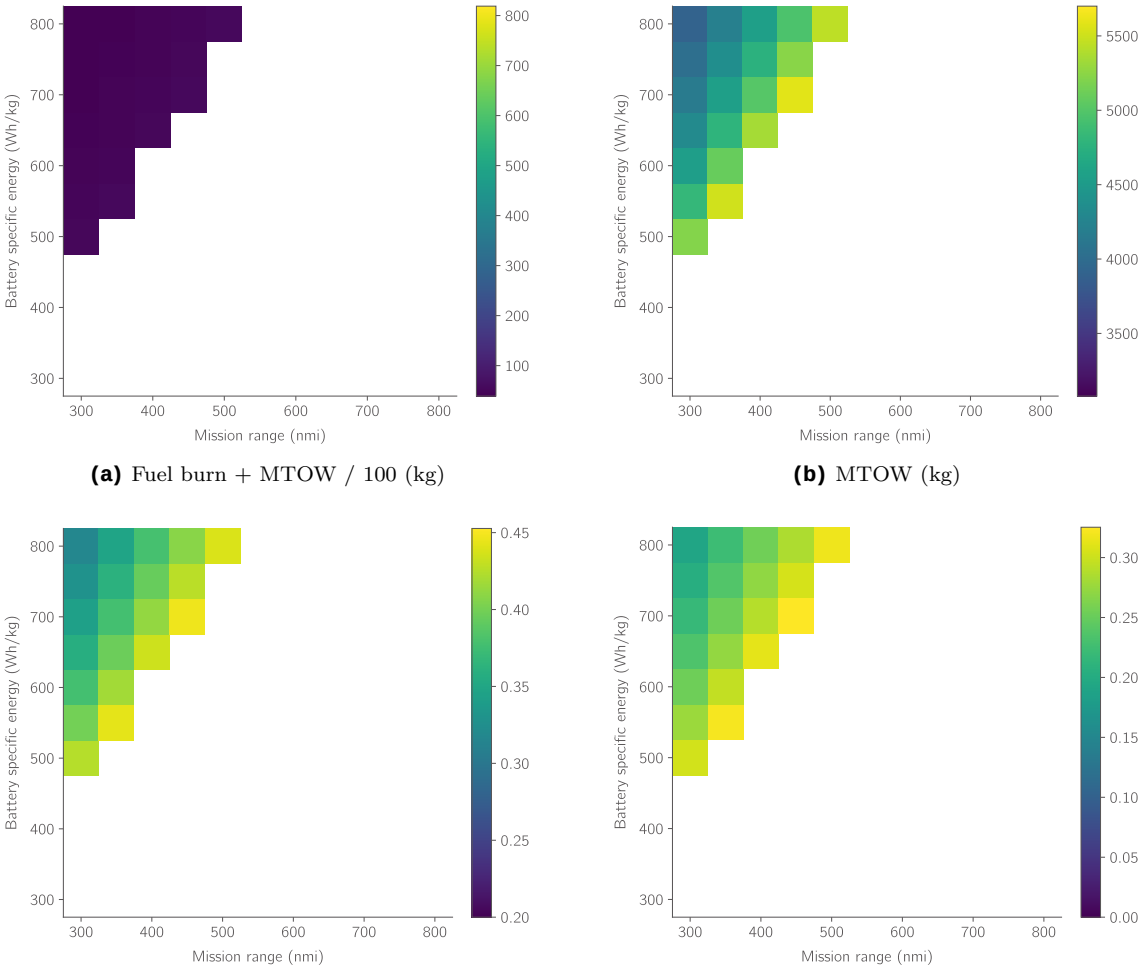

(a) Fuel burn + MTOW / 100 (kg)

(b) MTOW (kg)

(c) W_{PropSys} (including fuel and battery) / MTOW

(d) Battery weight / MTOW

Figure 6: All electric architecture MDO results.

4.2.3 Series Hybrid Architecture

Twin series hybrid optimization results are presented in Figure 7. The optimizer successfully optimizes the battery weight, electric motor and turboshaft rating, and cruise degree of hybridization to minimize the objective function for 97% of the cases. At a handful of long ranges and low battery specific energies, the optimizer fails to find a a combination of the design variables that meets the constraints (the MTOW bound in particular). This is partially due to the fact that the current simulation uses a hybridization of 0.4 in the other mission segments (takeoff, climb, and descent). Therefore, the optimizer is constrained by the energy requirements of those segments. To fly the longer range missions at a hybridization of 0.4 in takeoff, climb, and descent, the battery weight becomes so heavy that the aircraft exceeds the MTOW upper bound.

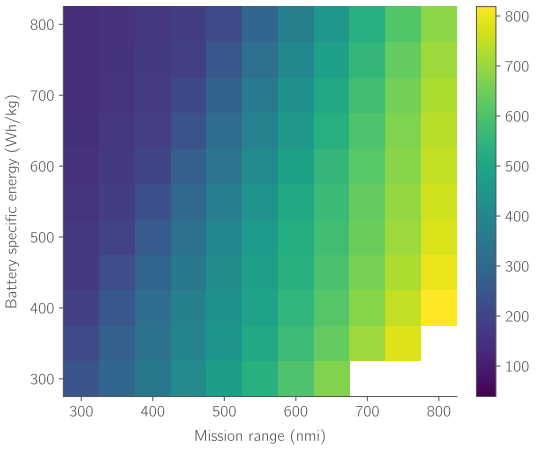

(a) Fuel burn + MTOW / 100 (kg)

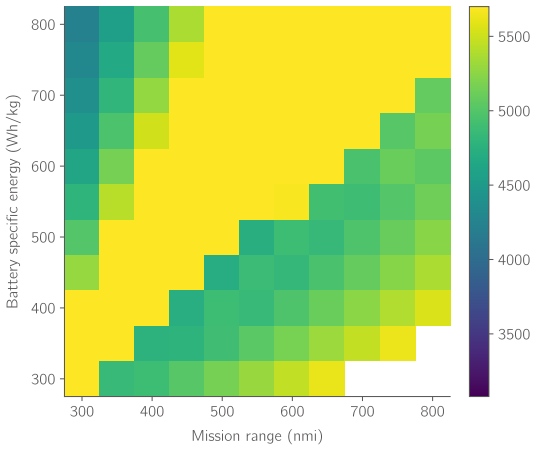

(b) MTOW (kg)

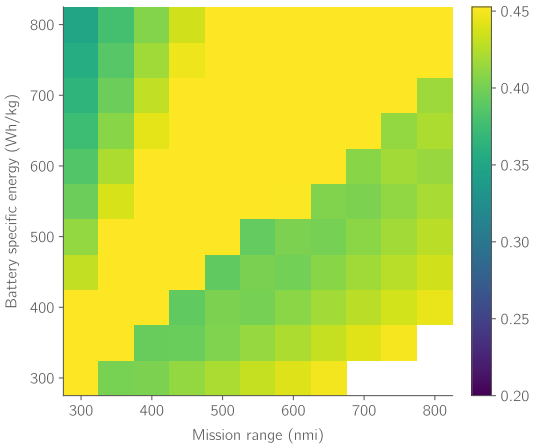

(c) $W_{PropSys}$ (including fuel and battery) / MTOW

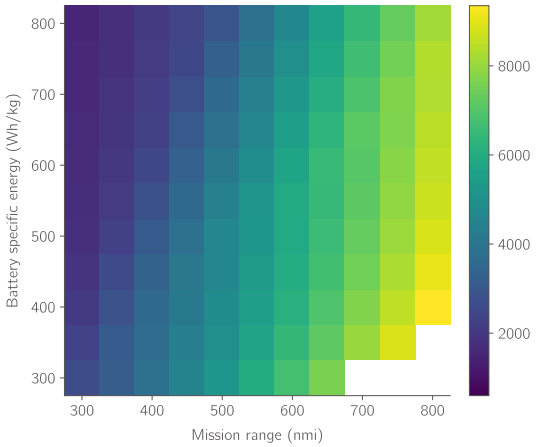

(d) Energy used (kWh)

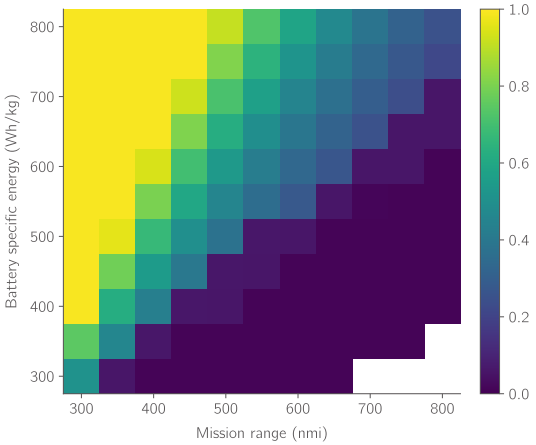

(e) Electrical DoH_{Cruise} (0 all fuel, 1 all electric)

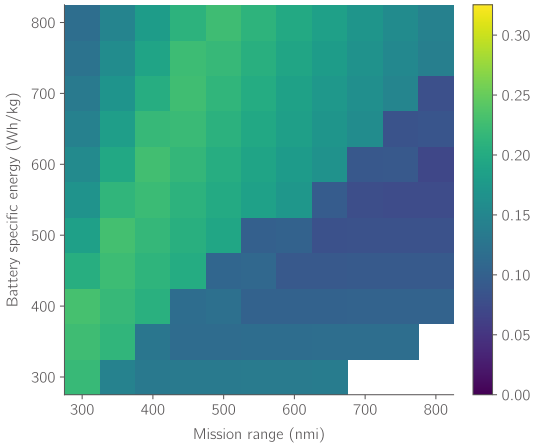

(f) Battery weight / MTOW

Figure 7: Series hybrid architecture MDO results.

In Figure 7e it is shown that at short ranges and high specific energies, the optimizer prefers to fly the mission completely on batteries. When the optimizer hits the upper bound of MTOW of 5,700 kg at 500 Wh/kg for a range of 350 nmi, it changes its strategy by supplementing the aircraft with just enough fuel to meet the required mission range without exceeding the MTOW bound. On the lower right of Figure 7e with high ranges and low specific energies, the optimizer prefers to fly the mission completely on fuel to reduce the battery weight as much as possible (hence reducing the MTOW portion of the objective function).

For all design points that use only fuel, the propulsion system weight (including battery and fuel weight) varies between 35 and 40% of the total aircraft weight. For points that use only batteries, it varies between 35 and 45% as shown in Figure 7c. The battery fraction follows a similar trend for the points on the upper left corner of the grid (all batteries) and lower right (all fuel) as shown in Figure 7f. At the design points that lie in the region around the diagonal of the grid, the MTOW is at the upper bound of 5,700 kg. For these design points (for example, at a range of 450 nmi and specific energy of 500 Wh/kg), the optimizer attempts to select the right combination of battery and fuel such that the MTOW does not exceed the upper limit while using as much battery power as possible. These results suggest that a hybrid configuration is only preferable when an upper bound on MTOW is present, a result also observed by Brelje [3].

4.2.4 Parallel Hybrid Architecture

Parallel hybrid optimization results are shown in Figure 8. The MDO results of the parallel hybrid architecture show similar trends to the series hybrid architecture. In the lower right region of Figure 8e, we see that the optimizer prefers to cruise completely on fuel to decrease MTOW and meet the design constraints. In the upper left region, the optimizer prefers to cruise fully on batteries. For parallel hybrid, the optimizer hits the upper bound on MTOW at 400 nmi with a battery specific energy of 500 Wh/kg. At this point, the aircraft has a mechanical DoH (the ratio of electric motor shaft power to total shaft power) of 92% with a battery weight of 1,627 kg. The optimizer sizes the electric motor and turboshaft rated powers to 370 and 539 kW, respectively. Beyond this point, the optimizer will replace the battery with fuel to meet the MTOW constraint. Therefore, at 450 nmi, the optimizer reduces the mechanical DoH to 78% and sizes the rated power of electric motor and engine to 311 and 453 kW. For both the 400 and 450 nmi cases at 500 Wh/kg the MTOW is at the upper bound of 5,700 kg, as shown in Figure 8b. This trend is similar to the series hybrid MDO results where the hybrid configuration is only preferable when an upper bound on MTOW is present.

An important point for the parallel hybrid architecture is how the sizing of the components' rated powers is performed. For the parallel hybrid, the throttle is applied on the sum of the rated powers of the turboshaft engine and electric motor. Thus, the parallel configuration tends to have a lower rated power of the electric motor at the same design point. For example, consider the case at 550 nmi and 550 Wh/kg. Both the series and parallel configurations have an MTOW of 5,700 kg. However, the parallel configuration has cruise mechanical DoH of 64% where the rated powers of the electric motor and turboshaft are 268 and 389 kW, respectively. For the series configuration at the same point, the cruise electric DoH (the ratio of batteries output electrical power to the total electrical power output) is 36% where the rated powers for the electric motor and turboshaft are 794 and 791 kW. In the parallel case, the turboshaft is used to generate mechanical shaft power to support the electric motor and deliver the required power to the propeller. In the series case, the turboshaft is used to generate the electric DC power needed to supply the power to the electric motors, which are used to generate all required shaft power.

The battery fraction reflects the selected degree of hybridization. At the 550 nmi and 550 Wh/kg design point, the DoH is 64% for the parallel and 36% for the series configuration. The weights of the batteries are 1,669 and 1,056 kg, respectively, accounting for 29% and 18% of the respective MTOWs as shown in Figures 8f and 7f. Even though there is a 600 kg difference in battery weight between the two configurations, the total weight of the respective propulsion systems are close at 2331 and 2198 kg, accounting for 41% and 39% of the respective aircraft models as shown in Figures 8c and 7c. This is due to the extra weight carried by the series hybrid configuration for the generator and converters.

4.3 Comparison of Architectures

The relative difference between the parallel and series hybrid architectures is presented in Figure 9. In addition, two design points are selected for comparison between all architectures, namely at ranges of 300 and 500 nmi both with a specific energy of 500 Wh/kg. The weight breakdown of selected architectures is presented in Figures 10 and 11. All design variables, assumptions, and optimization outputs are tabulated and presented in Table 2 along with the data of the reference aircraft model.

4.3.1 Series Hybrid Versus Parallel Hybrid Architectures

Figure 9b shows that out of 117 optimization cases, the parallel hybrid configuration has lower MTOW than the series hybrid at 107 design points. This is an expected result because the parallel architecture does not require the generator or rectifier required by the series architecture.

There are some cases on the grid's diagonal where both architectures have an MTOW at the 5,700 kg bound (gray in Figure 9b). These are the cases where the optimizer shifts from running the mission fully on batteries to using enough fuel to successfully run the mission without exceeding the MTOW bound. The reason the series hybrid configuration is lighter for 10 cases on the diagonal (highlighted in red) is the selection of the DoH by the optimizer. Because the parallel hybrid architecture has a fewer propulsion system components to carry than the series hybrid, it fill that weight with batteries and maintain a higher hybridization. For example, consider the case at 500 nmi and 450 Wh/kg. The parallel configuration has a cruise DoH of 56%, while the series hybrid has a cruise DoH of 5%. This variation in DoH leads to the parallel architecture to need a battery weight of 1,663 kg. The series configuration requires a battery weight of only 498 kg as it supplies 95% of the energy with fuel. This explains why the parallel architecture has a higher weight than series architecture in a handful of cases. The same patterns follows for the propulsion system weight fraction (including fuel and battery), as shown in Figure 9c. The parallel hybrid configuration has a lower propulsion system weight than the series configuration for most cases.

In addition to the parallel hybrid architecture being lighter, it also has fewer energy conversions in the power train design compared to the series architecture. These two factors result in lower energy consumption for the parallel hybrid configuration at all design points, as shown in Figure 9d. This suggests that for an aircraft similar to the King Air, the series hybrid architecture would require additional aerodynamic efficiency, structure design, or control benefits to be used at the investigated ranges and specific energies (e.g., distributed electric propulsion). Figure 9a shows that the parallel architecture leads to a more optimal design (based on our fuel burn + 0.01 MTOW objective function) at all design points.

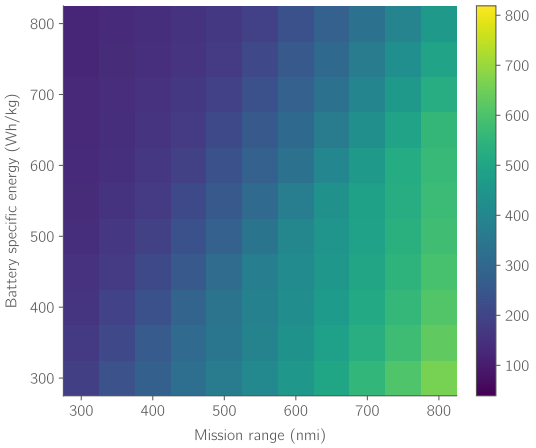

(a) Fuel burn + MTOW / 100 (kg)

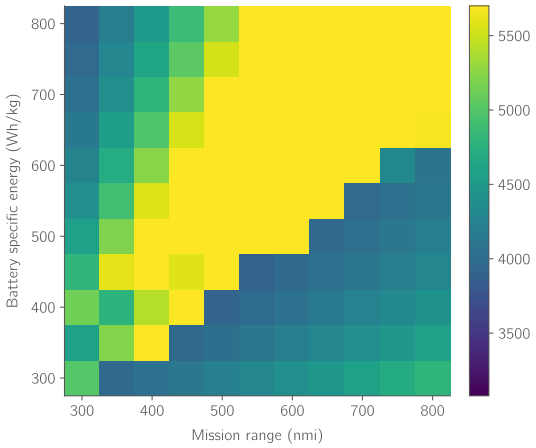

(b) MTOW (kg)

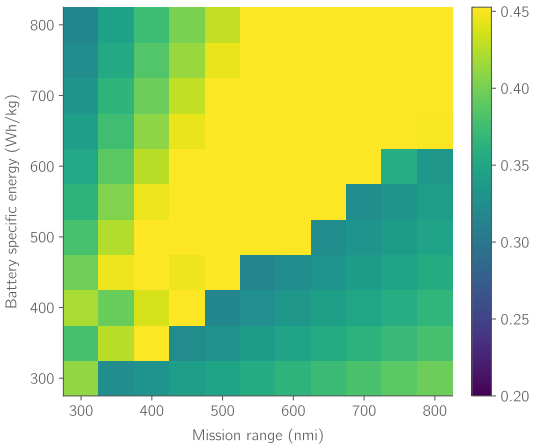

(c) W_{PropSys} (including fuel and battery) / MTOW

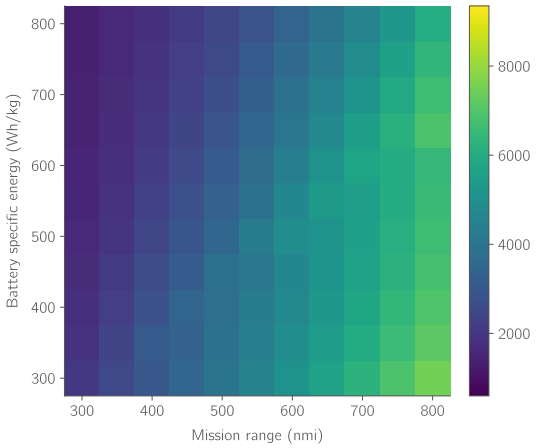

(d) Energy used (kWh)

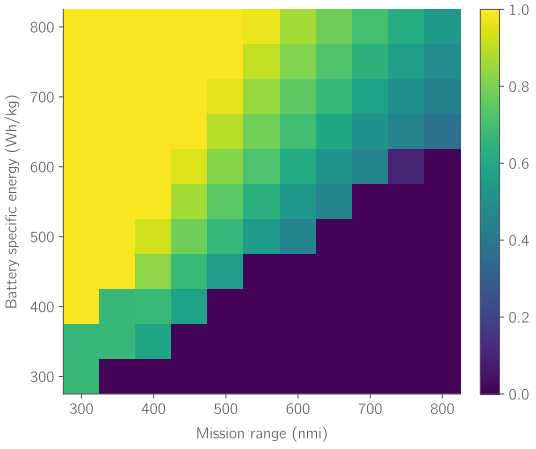

(e) Mechanical $\mathrm{DoH}_{\mathsf{Cruise}}$ (0 all fuel, 1 all electric)

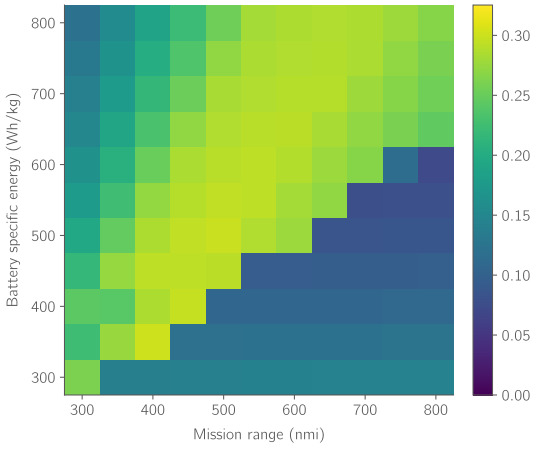

(f) Battery weight / MTOW

Figure 8: Parallel hybrid architecture MDO results.

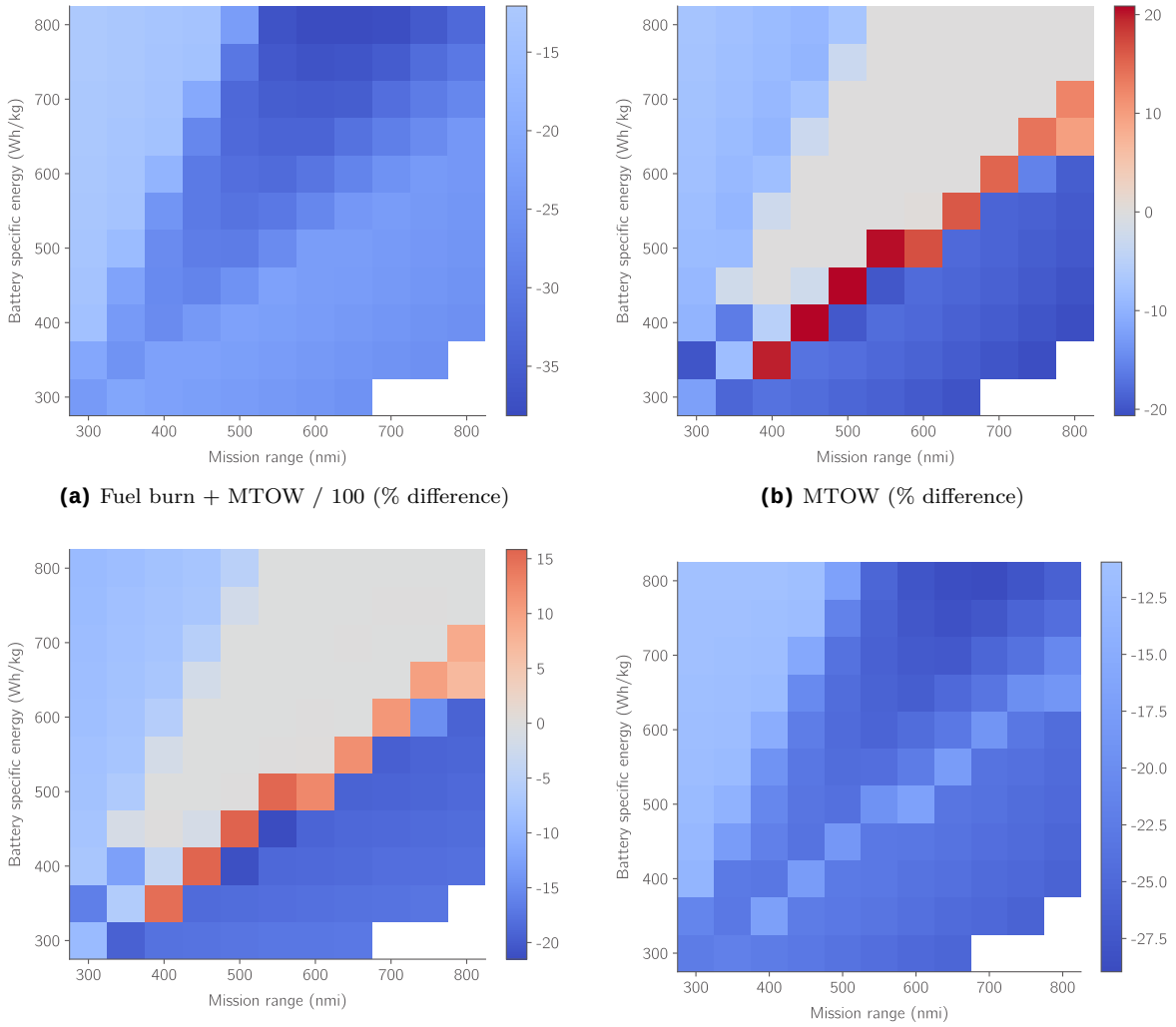

(a) Fuel burn + MTOW / 100 (% difference)

(b) MTOW (% difference)

(c) $W_{\texttt{PropSys}}$ (including fuel and battery) / MTOW (% difference)

(d) Energy used (% difference)

Figure 9: Parallel hybrid relative to series hybrid MDO architectures results. A positive (red) value indicates that the parallel hybrid quantity is greater than the series hybrid quantity.

4.3.2 Weight Breakdown

A weight breakdown for the five configurations at a mission range of 300 nmi and battery specific energy of 500 Wh/kg is shown in Figure 10. Figure 11 shows the same but at a mission range of 500 nmi. The conventional architecture has the lowest MTOW of all architectures for the two selected design points at a battery specific energy of 500 Wh/kg and for ranges of 300 and 500 nmi. The electric architecture's propulsion system weight fraction (excluding the battery) is the least among the five architectures on the 300 nmi and 500 Wh/kg mission due to its high efficiency and specific power. However, because of the electric architecture's high power requirements from having the greatest MTOW, the electric propulsion system's absolute weight (excluding the battery) is still greater than that of the conventional architecture (excluding fuel). For the short range of 300 nmi, the electrification of the reference aircraft has lead to an increase in MTOW compared to the conventional configuration of 69%, 62%, 48%, and 25% for the all electric, series hybrid, parallel hybrid, and turboelectric architectures, respectively.

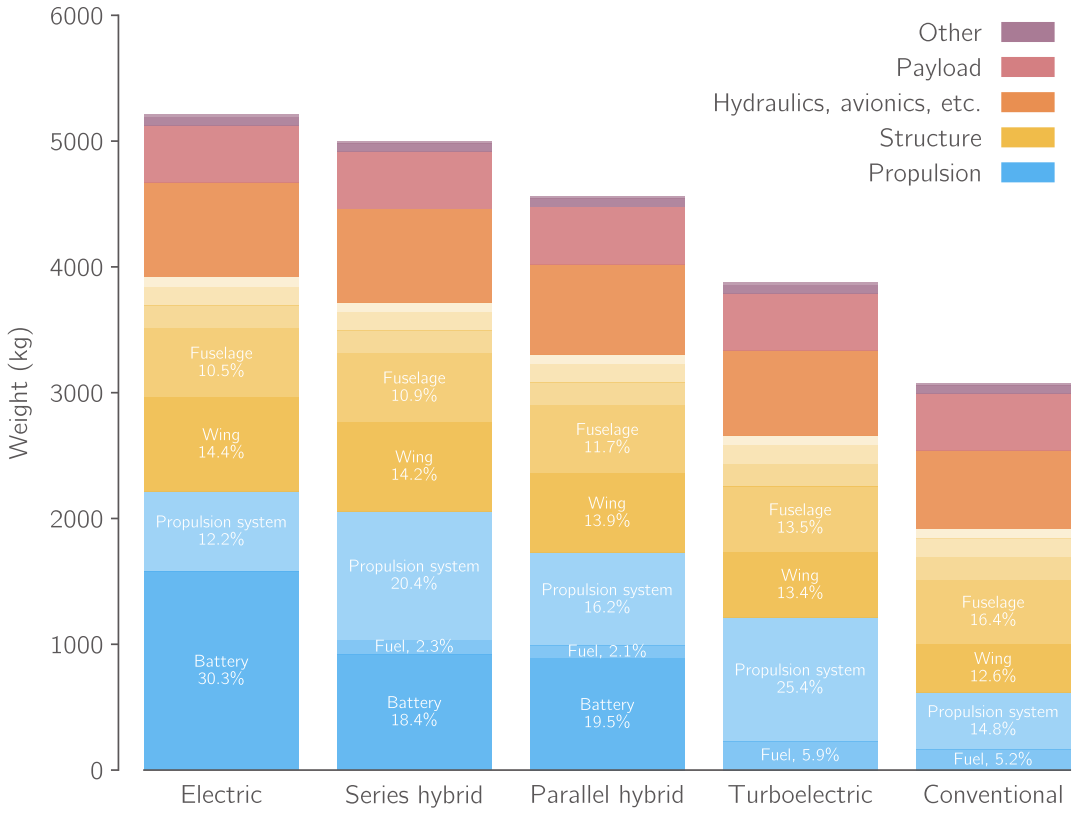

Figure 10: Weight breakdown for architectures at a mission range of 300 nmi and e_b of 500 Wh/kg.

A 200 nmi increase in the design mission range increases the MTOW of the conventional architecture by only 6%, from 3,079 kg to 3,259 kg as stated in Table 2. For other architectures, the percentage increase is greater. For example, the turboelectric architecture increases by 9%, series hybrid by 14%, and parallel hybrid by 25%. This is despite the transition of the hybrid architectures to lower hybridizations. There is no feasible solution for the all electric architecture at the higher range that meets the MTOW bound, so it is excluded.

From the discussion in Sections 4.2.3 and 4.2.4, we know that at moderate missions ranges and battery specific energies the optimizer uses as much battery as possible without exceeding the MTOW upper bound. At the 500 nmi and 500 Wh/kg case shown in Figure 11, both series and parallel architectures have a weight of 5,700 kg. However, because the parallel hybrid architecture has fewer propulsion system components to carry, it can fill up more weight with battery. As a result, the parallel architecture has a DoH of 67% with a battery weight of 1,696 kg, while the series architecture has a DoH of only 38% with a smaller battery weight of 1,099 kg. From the point of view of MTOW, the conventional architecture offers the best advantage of having the lowest weight at all design points.

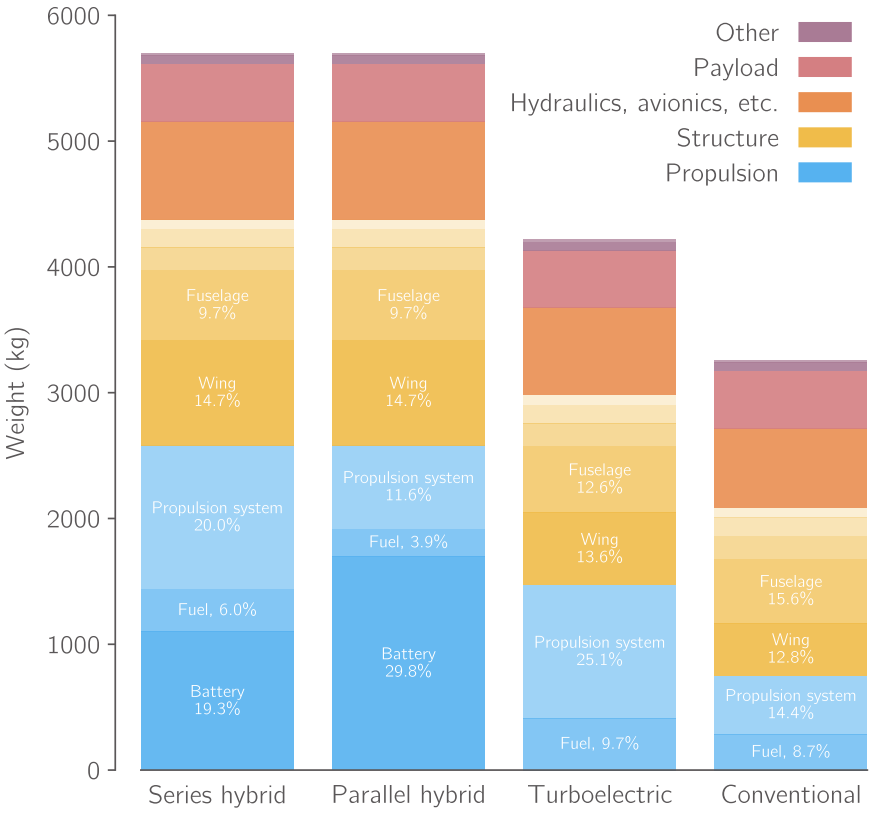

Figure 11: Weight breakdown for architectures at a mission range of 500 nmi and e_b of 500 Wh/kg.

5 Conclusions and Outlook

This paper presents an automated approach for propulsion architecture construction, integration, and quantitative aircraft-level evaluation. It introduces a prerequisite step for building flexible simulations to enable large architecture optimization studies. We use a function-based decomposition of the propulsion system components to allow modular and rapid definition of architectures. We demonstrate our approach by using it to investigate the electrification of a regional turboprop aircraft model.

Hundreds of individual MDO cases over a range of battery specific energies and mission ranges reveal nuanced trends in the hybrid architecture design space. In this case, hybrid propulsion is preferred over fuel-based and all electric architectures only when there is an upper limit on MTOW. The conventional architecture has the lowest MTOW among all architectures while the all electric architecture consumes the least energy at the investigated design points.

At the current technological level, turboelectric and series hybrid architectures are preferred only in cases when there is an additional aerodynamic efficiency, structural, or control benefit through technologies such as distributed electric propulsion. The fully electric architecture is only feasible for design ranges at or below 500 nmi with high battery specific energy. Note that the specific trends shown may not carry over to other cases, such as a clean sheet design.

Using the presented approach, researchers and designers can rapidly examine the tradespace for a wide variety of architectures with different missions and assumptions. Future work will include an architecture optimization study where the propulsion system architecting method is integrated in

the design optimization loop. This will use the Architecture Design and Optimization Reasoning Environment (ADORE) [6] to generate a Pareto set of architectures for given top-level aircraft requirements (TLARs). This work will use nested optimization to optimize the electric components and aircraft sizing in addition to the architecture. The current setup can also be connected to overall aircraft design tools to allow a higher fidelity analysis with different disciplines to produce a robust design.

Table 2: Baseline analysis and MDO results (mixed objective between minimum fuel burn and MTOW)

	Parameters	King Air C90GT (Model) [3]	King Air C90GT (Published) [3]	Conventional	Turboelectric	All Electric	Series Hybrid	Parallel Hybrid	Conventional	Turboelectric	Series Hybrid	Parallel Hybrid
Opt Problem Grid	Optimization Rules	Analysis	Analysis	MDO	MDO	MDO	MDO	MDO	MDO	MDO	MDO	MDO
	Specific Energy (Wh/kg)	-	-	-	-	500	500	500	-	-	500	500
	Design Range (nmi)	1,000	894+100	300	300	300	300	300	500	500	500	500
Design Variables	MTOW (kg)	4,581	4,581	3,079	3,876	5,212	5,001	4,563	3,259	4,218	**5,700**	**5,700**
	Mech Turboshaft (kW, for each)	405	405	420	-	-	-	464	444	-	-	389
	Elec Motor (kW, for each)	-	-	-	-	727	698	319	-	590	794	268
	Elec Turboshaft (kW)	-	-	-	902	-	695	-	-	980	791	-
	Prop Diameter (m)	2.29	2.29	**2.2**	**2.2**	**2.2**	**2.2**	**2.2**	**2.2**	**2.2**	**2.2**	**2.2**
	Battery Wt (kg)	-	-	-	-	1,579	921	891	-	-	1,099	1,696
	DoH at cruise	-	-	-	-	-	**99%**	**99%**	-	-	38%	67%
Weights	OEW (kg)	3,255	3,255	2,465	3,195	4,758	4,434	4,013	2,523	3,354	4,907	5,024
	Design Payload (kg)	454	454	454	454	454	454	454	454	454	454	454
	Propulsion System Weight (kg)	-	-	456	986	2,215	1,943	1,632	469	1,059	2,241	2,358
	Propulsion System Fraction (%)	-	-	14.8	25.4	42.5	38.8	35.8	14.4	25.1	39.3	41.4
	Battery Fraction (%)	-	-	-	-	30.3	18.4	19.5	-	-	19.3	30.0
Wing Geometry	Wing Ref Area (m^2)	27.3	27.3	18.4	23.1	31.1	29.8	27.2	19.4	25.1	34.0	34.0
	Wingspan (m)	15.3	15.3	12.6	14.1	16.3	16.0	15.3	12.9	14.7	17.1	17.1
	Aspect Ratio	8.58	8.58	8.58	8.58	8.58	8.58	8.58	8.58	8.58	8.58	8.58
	Wing Loading (kg/m^2)	167.8	167.8	167.8	167.8	167.8	167.8	167.8	167.8	167.8	167.8	167.8
Aerodynamics	Flaps-Down C_{Lmax}	1.52	-	1.52	1.52	1.52	1.52	1.52	1.52	1.52	1.52	1.52
	Oswald Efficiency	0.80	-	0.80	0.80	0.80	0.80	0.80	0.80	0.80	0.80	0.80
	C_{D0} at Cruise	0.0220	-	0.0220	0.0220	0.0220	0.0220	0.0220	0.0220	0.0220	0.0220	0.0220
	C_{D0} at Takeoff	0.0290	-	0.0290	0.0290	0.0290	0.0290	0.0290	0.0290	0.0290	0.0290	0.0290
Performance	Takeoff Rotation Speed (KIAS)	89.8	90	89.8	89.8	89.8	89.8	89.8	89.8	89.8	89.8	89.8
	Climb Rate (ft/min)	1,500	-	1,500	1,500	1,500	1,500	1,500	1,500	1,500	1,500	1,500
	Climb Speed (KIAS)	124	-	124	124	124	124	124	124	124	124	124
	Cruise Speed (KIAS)	170	170	170	170	170	170	170	170	170	170	170
	Cruise Altitude (ft)	29,000	29,000	29,000	29,000	29,000	29,000	29,000	29,000	29,000	29,000	29,000
	Descent Rate (ft/min)	600	-	600	600	600	600	600	600	600	600	600
	Descent Speed (KIAS)	130	-	140	140	140	140	140	140	140	140	140
	BFL,SL,ISA+0 (ft)	**4,452**	**4,452**	**4,452**	**4,452**	**4,452**	**4,452**	**4,452**	**4,452**	**4,452**	**4,452**	**4,452**
Evaluation Outputs	Fuel burn + 0.01MTOW	-	-	191	266	52	164	142	315	452	397	279
	Mission Fuel burn (kg)	728.4	-	160	227	0.0	114	96.3	283	410	340	222
	Total Energy used (kWh)	-	-	1,917	2,715	789	1,819	1,596	3,377	4,903	4,606	3,500

Bold numbers indicate an active constraint, an upper or lower bound.

6 Contact Author Email Address

The authors would like to invite interested potential collaborators to contact the corresponding authors, mailto: Jasper.Bussemaker@dlr.de, Mahmoud.Fouda@dlr.de, eytana@umich.edu

7 Copyright Statement

References

[1] UN climate change conference, 2019. URL https://unfccc.int/cop25.

[2] Eytan J. Adler, Benjamin J. Brelje, and Joaquim R. R. A. Martins. Thermal management system optimization for a parallel hybrid aircraft considering mission fuel burn. *Aerospace*, 9 (5), 2022. ISSN 2226-4310. doi: 10.3390/aerospace9050243. URL https://www.mdpi.com/2226-4310/9/5/243.

[3] Benjamin J. Brelje and Joaquim R. R. A. Martins. Development of a conceptual design model for aircraft electric propulsion with efficient gradients. In *2018 AIAA/IEEE Electric Aircraft Technologies Symposium*, Reston, Virginia, 2018. American Institute of Aeronautics and Astronautics. ISBN 978-1-62410-572-2. doi: 10.2514/6.2018-4979.

[4] Benjamin J. Brelje and Joaquim R. R. A. Martins. Electric, hybrid, and turboelectric fixed-wing aircraft: A review of concepts, models, and design approaches. *Progress in Aerospace Sciences*, 104:1–19, 2019. ISSN 03760421. doi: 10.1016/j.paerosci.2018.06.004.

[5] J. H. Bussemaker, P. D. Ciampa, and B. Nagel. System architecture design space modeling and optimization elements. In *32nd Congress of ICAS*, 2021. URL https://www.icas.org/ICAS_ARCHIVE/ICAS2020/data/preview/ICAS2020_0203.htm.

[6] J. H. Bussemaker, L. Boggero, and P. D. Ciampa. From system architecting to system design and optimization: A link between mbse and mdao. In *INCOSE International Symposium*, June 2022.

[7] Jasper H. Bussemaker, Pier Davide Ciampa, and Bjoern Nagel. System architecture design space exploration: An approach to modeling and optimization. In *AIAA AVIATION 2020 FORUM*, Reston, Virginia, 2020. American Institute of Aeronautics and Astronautics. ISBN 978-1-62410-598-2. doi: 10.2514/6.2020-3172.

[8] Jasper H. Bussemaker, Thibault de Smedt, Gianfranco La Rocca, Pier Davide Ciampa, and Björn Nagel. System architecture optimization: An open source multidisciplinary aircraft jet engine architecting problem. In *AIAA AVIATION 2021 FORUM*, Reston, Virginia, 2021. American Institute of Aeronautics and Astronautics. ISBN 978-1-62410-610-1. doi: 10.2514/6.2021-3078.

[9] Gustavo. Esdras and Susan. Liscouet-Hanke. Development of core functions for aircraft conceptual design: methodology and results. In *Canadian Aeronautics and Space Institute AERO*, Montreal, Canada, 2015. URL https://www.researchgate.net/publication/277021129_Development_of_Core_Functions_for_Aircraft_Conceptual_Design_Methodology_and_Results/citations.

[10] Philip E. Gill, Walter Murray, and Michael A. Saunders. SNOPT: An SQP algorithm for large-scale constrained optimization. *SIAM Review*, 47(1):99–131, 2005. doi: 10.1137/S0036144504446096.

[11] Justin S. Gray, John T. Hwang, Joaquim R. R. A. Martins, Kenneth T. Moore, and Bret A. Naylor. Openmdao: an open-source framework for multidisciplinary design, analysis, and optimization. *Structural and Multidisciplinary Optimization*, 59(4):1075–1104, 2019. ISSN 1615-147X. doi: 10.1007/s00158-019-02211-z.

[12] David S Lee, DW Fahey, Agnieszka Skowron, MR Allen, Ulrike Burkhardt, Q Chen, SJ Doherty, S Freeman, PM Forster, J Fuglestvedt, et al. The contribution of global aviation to anthropogenic climate forcing for 2000 to 2018. *Atmospheric Environment*, 244:117834, 2021.

[13] Giuseppe Palaia, Davide Zanetti, Karim Abu Salem, Vittorio Cipolla, and Vincenzo Binante. Thea-code: a design tool for the conceptual design of hybrid-electric aircraft with conventional or unconventional airframe configurations. *Mechanics & Industry*, 22:19, 2021. ISSN 2257-7777. doi: 10.1051/meca/2021012.

[14] Higor L. Silva, Gustavo J. Resende, Roberto M. C. Neto, André R. D. Carvalho, Alexandre A. Gil, Mateus A. A. Cruz, and Thiago A. M. Guimarães. A multidisciplinary design optimization for conceptual design of hybrid-electric aircraft. *Structural and Multidisciplinary Optimization*, 64(6):3505–3526, 2021. ISSN 1615-147X. doi: 10.1007/s00158-021-03033-8.

[15] Neil Wu, Gaetan Kenway, Charles A. Mader, John Jasa, and Joaquim R. R. A. Martins. pyoptsparse: A python framework for large-scale constrained nonlinear optimization of sparse systems. *Journal of Open Source Software*, 5(54):2564, 2020. doi: 10.21105/joss.02564.

[16] J. Zamboni. *A method for the conceptual design of hybrid electric aircraft.* M.sc. thesis, 2018. URL https://repository.tudelft.nl/islandora/object/uuid%3A7b7dc56b-6647-4cc9-98f6-2ed5d488c759.

Appendix

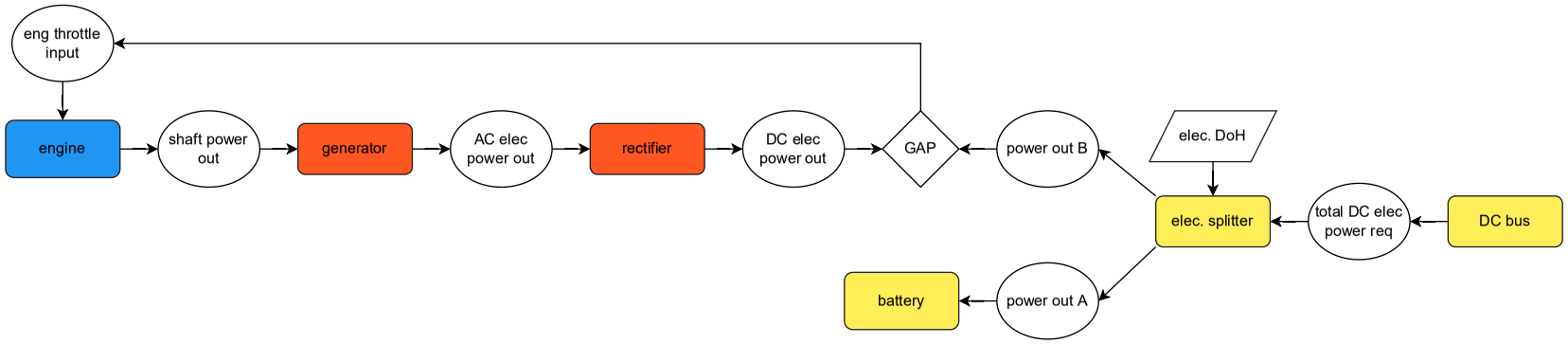

Figure 12: Series hybrid architecture electric power generation implementation with electrical DoH separating the power load requirement between the engine chain and the battery. The engine throttle is found using an implicit solver to match the power values on both sides of the implicit gap.

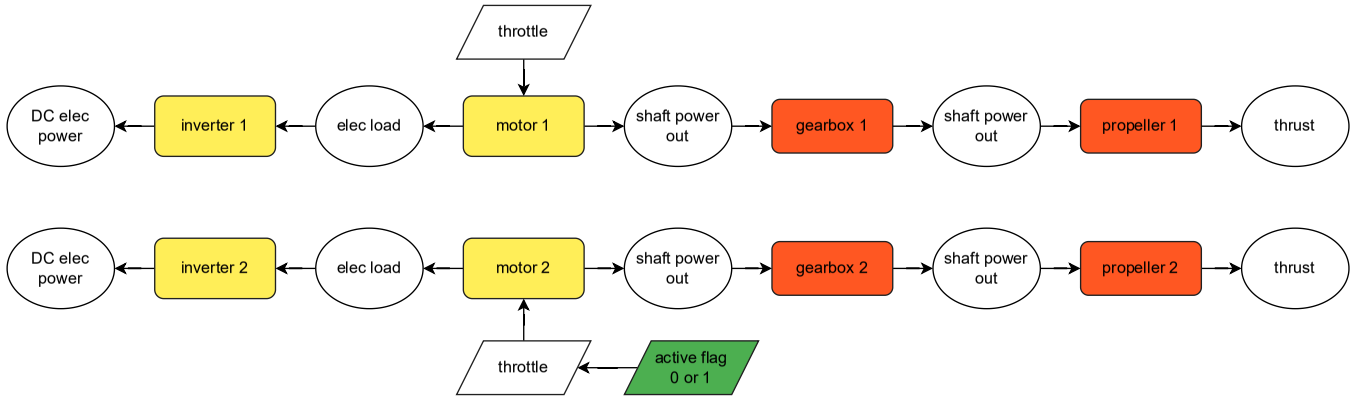

Figure 13: Series hybrid architecture mechanical power and thrust generation elements with one engine inoperative (OEI) applied on the second electric motor component. During OEI, the throttle input to the second motor is zero and it is assumed as a failed motor with no power output and no electric load output.

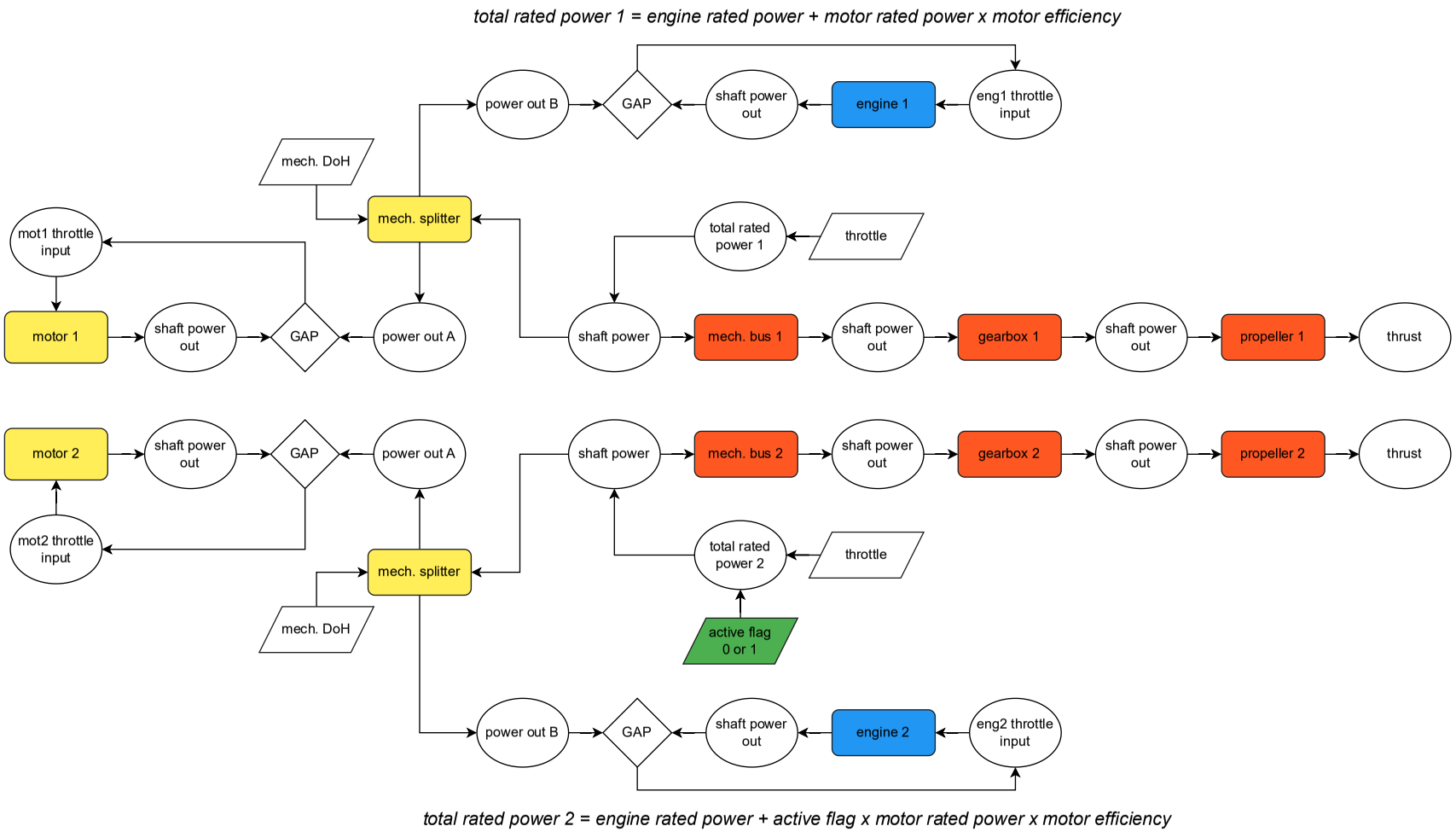

Figure 14: Parallel hybrid architecture mechanical power and thrust generation elements implementation with One Engine Inoperative (OEI) applied on the second electric motor component. The mechanical splitter separates the shaft power requirement to A and B based on the design mechanical DoH. The motor rated power is sized such that it can provide the power required A at all points during the mission and similarly the engine rated power is sized such that it can supply the power required B. When OEI is active, the required power A becomes zero and the second electric motor has failed with no power output and no electric load. Therefore, the total rated power available for the second branch is equal to only the engine rated power. A solver is used to find the throttle inputs such that the power values on both sides of the implicit gap is equal.